A REAL-TIME PEDESTRIAN DETECTION SYSTEM IN STREET SCENE

Ai-ying Guo[1], Mei-hua Xu[1, 2], Feng Ran[3], Qi Wang[3]

[1] School of Mechatronics Engineering and Automation, Shanghai University, 200072, Shanghai, P.R.C

[2] Department of Electrical and Mechanical Engineering, Shan Xi Light Industry and Technical College, 030013, Shanghai, P.R.C

[3] Microelectronics Research and Development Center, Shanghai University, 200072, Shanghai, P.R.C

Emails: gayshh@shu.edu.cn; mhxu@shu.edu.cn; ranfeng@shu.edu.cn;175858895@qq.com

Submitted: Apr 17, 2016 ***Accepted: Aug. 1, 2016*** ***Published: Sep. 1, 2016***

Abstract-Pedestrian detection is the key technology in Advanced Driver Assistant System (ADAS).Until recently, pedestrian detection, which is realized as the vehicle equipment, still doesn't have the mature product. So, this thesis proposes a novel pedestrian detection system on board with the E-HOG (Histogram of Gradient) IP (intellectual property), can be used as the real time vehicle equipment. Three contributions are made in this thesis. Firstly, Sobel operator cascaded Uniform Local Binary Pattern (LBP) and E-HOG is the novel structure of pedestrian detection system. The Sobel operator gives the sliding step of Uniform LBP detection window, without using the results of LBP detection window. Through this operation, the detection speed will be improved. Second, the vehicle equipment of pedestrian detection is self-developed using FPGA as core devices. Third, E-HOG IP, which is promoted based on the HOG, can extract pedestrian or other objects feature. Without sacrifice of accuracy, this pedestrian detection on board deals with 30 fps (640x480 pixels) and can be used as the real-time detection system.

Index term: Pedestrian Detection; Real-Time; Street Screen; Sobel; LBP; E-HOG; Accelerator; IP; Vehicle equipment

I. INTRODUCTION

One of the main causes of fatality all over the world is the road accidents. These accidents come out a massive economic cost on the government and people. So, numerous researchers and automobile manufactures with strong affinity for functional surround view cameras study the Advanced Driver Assistance System(ADAS).The goal of ADAS is to achieve zero fatalities through an active or passive safety system[1][2]. Pedestrian detection is a key technology in ADAS. After several years of development, pedestrian detection now exhibit many efficient algorithms. Covariance matrices [3], Like-Haar [4], Multi-feature [5], Histogram of gradient (HOG) [6], DPM [7], Sparse coding [8] and Convolutional Neural Network CNN [9] are well known algorithms for extracting pedestrian feature. Nevertheless, Boosting [10] , Support Vector Machine (SVM) [11][12] and MRF [13] are also most frequently used to classify whether pedestrian zone or not.

But the command point is that many researchers improve the performance of pedestrian detection system by proposing more complicated algorithms or transplanting to better hardware platform. Despite the good performances of these systems, due to the complex background and variable contour lines in the pedestrian, the problems of pedestrian detection is that real-time and accuracy can’t balance very well in the vehicle equipment. Such as, Oncel et al. utilize complicated covariance matrices as feature descriptors for extracting pedestrians' feature. The d-dimensional non-singular covariance matrices can be represented as a connected Riemannian manifold. This algorithm used for pedestrian detection can reach 99.8 percent at the specified detection and 35.8 percent at the rejection rates on Daimler data set [3]. Benenson et al. speed up the processing speed from testing to training time based on CPU with GPU desktop machine [14]. This well-known monocular system can deal with 135 fps. Others, pedestrian detection systems sometimes are utilized by FPGA with CPU or GPU. Bauer et al. designs the pedestrian detection structure that incorporates FPGA for feature extraction and GPU for classification on the desktop, which can handle 640x480 pixels under 100ms [15]. But, if these algorithms or systems have the huge drawback to be transplanted into the hardware system: huge computation and memory, which aren’t suited as vehicle equipment.

So in order to solve these problems, this thesis proposes a unify framework and designs the hardware system with the E-HOG IP. Three contributions are made in this paper.

(1)To find a better solution about the pedestrian detection on board, a unify structure for pedestrian detection is designed: Sobel operator cascaded Uniform LBP and E-HOG based on the Linear-SVM. This structure of pedestrian detection is divided into three stages. Sobel operator is used to calculate the steps of sliding window as the first stage in this system. According to sliding step, the Uniform LBP is used to extract Regions Of Interest (ROIs). The E-HOG, which is the promote HOG, determines whether pedestrian zone or not in the last stage.

(2)The vehicle equipment of pedestrian detection system using FPGA is developed. This hardware includes one FPGA, three SDRAMs, one camera and some other interfaces.

(3) In order to decrease the hardware overload and improve detection speed, the E-HOG IP is designed, and can be used as the accelerator for this detection system on board.

The experiment shows that this pedestrian detection with E-HOG IP can process 30 fps and satisfy the real-time without using GPU or CPU. This is the low-cost vehicle equipment for pedestrian detection.

The organization is designed as follows. After a general introduction of the pedestrian detection, the unify structure of pedestrian detection is explained in section II. The pedestrian detection on board will be discussed in section III. In section IV, the evaluation of E-HOG IP, system and vehicle equipment has been presented. The lecture has been concluded in section V.

II. RELATED THEORY OF PEDESTRIAN DETECTION

2.1 Region Location through Sobel operator

Sobel operator is the effective descriptor for edge detection. It is actually the first order discrete operator and calculates the similarity of image gray. The convolution factor is showed in the function (1) and (2).

$$S_x = \begin{bmatrix} 1 & 2 & 1 \\ 0 & 0 & 0 \\ -1 & -2 & -1 \end{bmatrix} \quad (1)$$

$$S_y = \begin{bmatrix} 1 & 0 & -1 \\ 2 & 0 & -2 \\ 1 & 0 & -1 \end{bmatrix} \quad (2)$$

In order to decrease the calculation, the function (3) generates the gradient value.

$$S = |S_x| + |S_y| \quad (3)$$

Figure1. (a) is the original image; Figure1.(b) is the gray image.

The threshold value is used to calculate the Sobel value. If the Sobel gradient value is bigger than the threshold, this pixel will be set 1.If the value is smaller, this pixel will be set 0. After this operation, the Sobel image will be generated, as Figure 1. (c) Shows.

(a) Original Image

(b) Graying Image

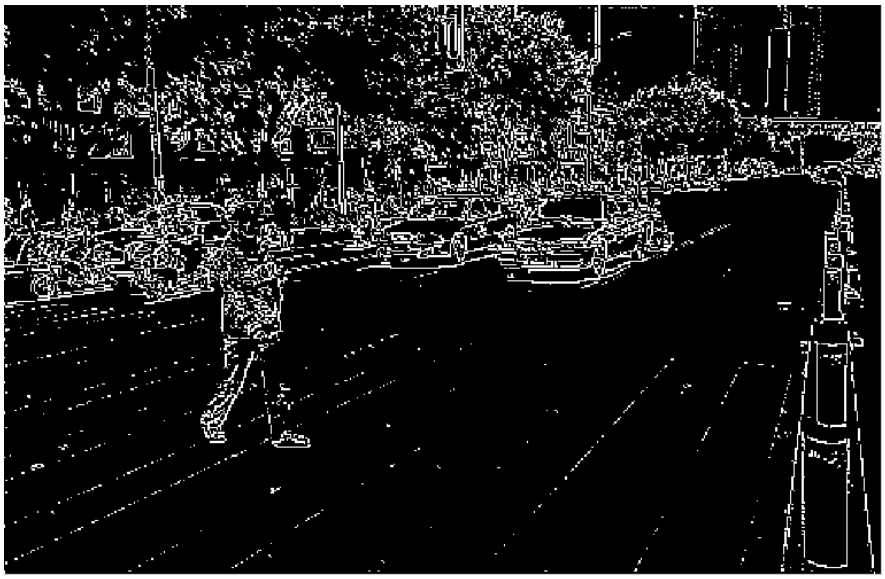

(c) Sobel Image

Figure .1 Different images

Because the Sobel operator isn't suited to human vision, it is difficult to detect pedestrians directly. In this paper, the Sobel operator is used to calculate the margin gray. The whole Sobel image will be divided into the 8x8 pixels as one block .The corresponding block has no overlap. In function (4), $S(i, j)$ stands for the Sobel value and (m, n) for the serial numbers in one block; $S(i, j)$ is 1 or 0; $SI(m,n)$ is the integral Sobel value in one block.

$$SI(m,n) = \sum_{i,j=1}^{i,j=4} S(i, j) \quad (4)$$

Let's suppose V_1 and V_2 stand for the different threshold integral values. When $SI(m,n) \geq V_1$ and $SI(m,n) \leq V_2$, it means that this location has the edge change and may be the pedestrians zone. Two adjacent blocks are used to calculate the sliding step of detection window. So, the top left of these two blocks is also the top left of one detection window in the second stage. If don't satisfy the thresholds, the top left is not. The smallest step of second stage detection window is 4 pixels. If the integral value satisfies the different threshold values, the distance of the Uniform LBP detection window will be 4 pixels to the last detection window. If not, the step is the addition from the $S_{original}$ and 4 pixels, which $S_{original}$ stands for step size of last detection window. The strategy is calculated according to the function (5).

$$S_{original} = \begin{cases} 4, & SI(m,n) \geq V_1, SI(m,n) \leq V_2 \\ S_{original+4,else} \end{cases} \quad (5)$$

Sobel operator replaces the Uniform LBP with Linear SVM to determine the detection window step. The block of Sobel operator is 4x4 pixels and detection window of LBP is about 64x128 pixels. Compared with the calculation of Uniform LBP in one detection window, o (4x4x2+17) of Sobel Operator is smaller than o (64x128+59).So the speed of detection will be improved. (The experiment will be given in § 4.2.)

2.2 E-HOG with high-speed

Thought of E-HOG is that the body shape is described through gradient and marginal density orientation. Let's suppose $H(x,y)$ is for the pixel value of (x, y).Then, the gradient of (x, y) are calculated by function (6).

$$\begin{cases} G_x(x,y) = H(x+1,y) - H(x-1,y) \\ G_y(x,y) = H(x,y+1) - H(x,y-1) \end{cases} \quad (6)$$

Next step is to generate the magnitude and orientation of pixel. $M(x,y)$ stands for the magnitude and $\theta(x,y)$ for the orientation.

$$M(x,y) = \sqrt{G_x(x,y)^2 + G_y(x,y)^2} \quad (7)$$

$$\theta(x,y) = \arctan(\frac{G_y(x,y)}{G_x(x,y)}) \quad (8)$$

Third step is to construct the histogram using magnitude and orientation, called tri-linear interpolation.

$$h(x_1,y_1,\theta_1) \leftarrow h(x_1,y_1,\theta_1) + M(x,y)(1-\frac{y-y_1}{dy})(1-\frac{x-x_1}{dx})(1-\frac{\theta(x,y)-\theta_1}{d\theta}) \quad (9)$$

$$h(x_1,y_1,\theta_2) \leftarrow h(x_1,y_1,\theta_2) + M(x,y)(1-\frac{y-y_1}{dy})(1-\frac{x-x_1}{dx})(1-\frac{\theta(x,y)-\theta_2}{d\theta}) \quad (10)$$

In function (9) and (10), $(1-\frac{x-x_1}{dx})$ and $(1-\frac{y-y_1}{dy})$ is the distance to the center of block; $(1-\frac{\theta(x,y)-\theta_2}{d\theta})$ and $(1-\frac{\theta(x,y)-\theta_1}{d\theta})$ is the distance to the center of corresponding bin, $h(x_1,y_1,\theta_1)$ for the histogram value of (x_1,y_1,θ_1). In order to promote the processing speed, the tri-linear interpolation will be redesigned.

About the orientation, the orientation is projected into 1 bin. According to this theory, function (9) and (10) are changed to:

$$h(x_1, y_1, \theta_1) \leftarrow h(x_1, y_1, \theta_1) + M(x, y)(1 - \frac{y - y_1}{dy})(1 - \frac{x - x_1}{dx}), if\ (\theta(x, y) \in \theta_1) \quad (11)$$

The location projections are changed with the corresponding distance to block center. Let's suppose one cell is divided into dash line zone and stone line zone as Figure.2 shows.

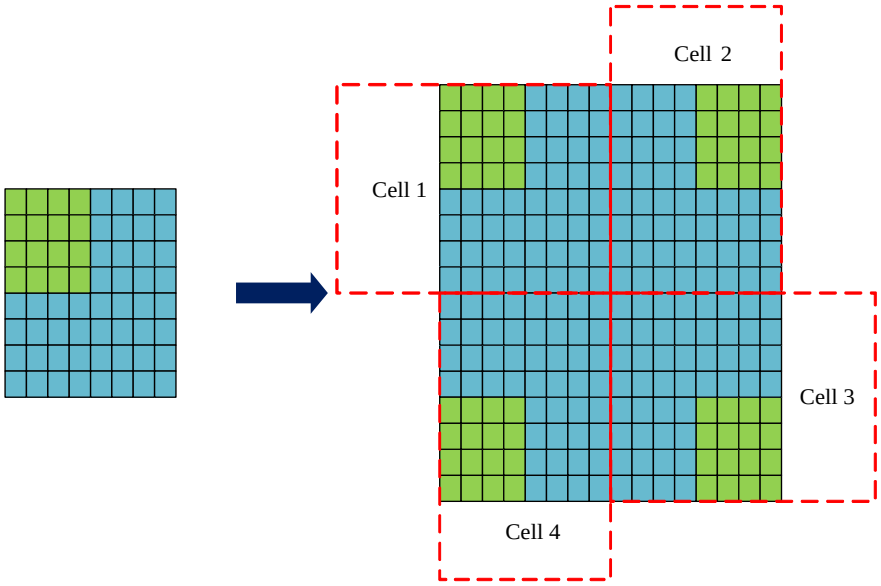

Figure.2 Different zone in one block

If one pixel locates in the dash line zone, then the function (10) is reviewed by the function (11). The magnitude of one pixel will make contribution to the other three cells in one block. If one pixel locates in the stone line, then the function (10) is changed to the function (12). The magnitude of one pixel, which locates in this zone, just makes the contribution to its own block, which is located.

$$h(x_1, y_1, \theta_1) \leftarrow h(x_1, y_1, \theta_1) + M(x, y)(1 - \frac{y - y_1}{dy})(1 - \frac{x - x_1}{dx}), if\ (\theta(x, y) \in \theta_1) \quad (12)$$

$$h(x_1, y_1, \theta_1) \leftarrow h(x_1, y_1, \theta) + M(x, y), if\ (\theta(x, y) \in \theta_1) \quad (13)$$

The histogram of E-HOG is constructed by function (14):

$$H_i = \sum_{x,y} I(h(x_1, y_1, \theta)) \in \theta_i), i = 1, 2, 3, \cdots, \ 9 \quad (14)$$

Last operation of E-HOG is the normalization. L1-norm, L2-norm and L1-sqrt are the methods to normalize the features. In E-HOG, the L2-norm is adopted.

$$f = \frac{v}{\sqrt{\|v\|_2^2 + e^2}} \quad (15)$$

2.3 Proper Classifier in the pedestrian detection

Classifier is also the key module for pedestrian detection. In pedestrian detection, Support Vector Machine (SVM) always is used as the classifier. SVM uses kernel function (Figure.3 showed) to map these huge features to high dimension vector. Then the vector can be separated by the plane.

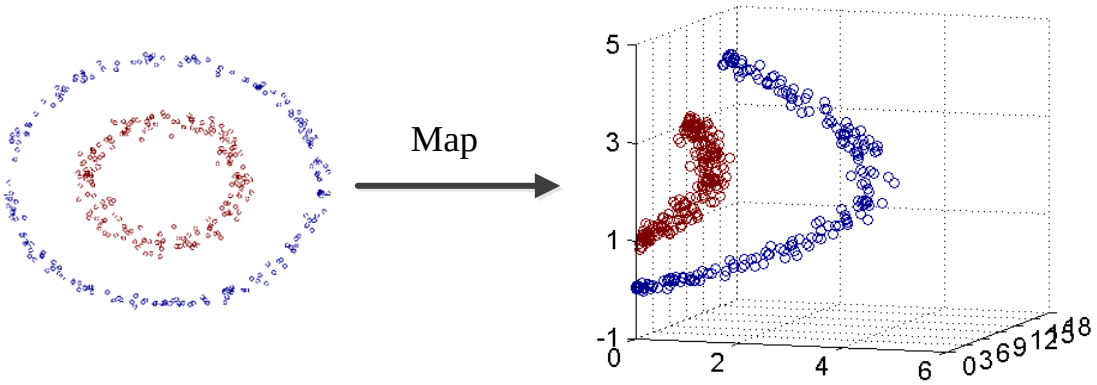

Figure.3 Map through kernel function

According to the different kernel function, SVM is designed with the different names and function. In this thesis, the Linear SVM is adopted in this paper. The kernel function in Linear SVM is defined as:

$$K(x_1, x_2) = \langle \varphi(x), \phi(y) \rangle \quad （16）$$

Then, the function of Linear SVM is expressed by:

$$f(x) = \sum_{i=1}^{l} \alpha_i y_i \langle \varphi(x), \phi(y) \rangle + b \quad (17)$$

2.4 Three stages for real-time pedestrian detection system

A novel structure of pedestrian detection system is designed with three stages: Sobel operation as first stage, LBP as second stage, and E-HOG as last stage, which is showed in Figure.4. Because the LBP and Uniform LBP theory are discussed in many papers, we won't explain any more [16] [17] [18].

In Figure.4, the frames are firstly scaled and sheared to extract the effective zone of one image. Then, the Sobel operator in first stage is used to deal with the effective zone. Sobel operators with different threshold values, calculate the step size of detection window, which is the LBP detection window. The threshold values are 3 and 10 separately. If the result is true, this size is the sliding size of detection window in second stage. If not, the step size will be recalculated. The Uniform LBP with SVM in second stage disposes 70% non “Pedestrian” zone and give the “Pedestrian” zone to the third stage. In third stage, E-HOG with SVM gives the finally result whether pedestrian zone or not. Because the whole image is scanned, one pedestrian will be blocked more than one window. Non-maximum suppression (NMS) is used to eliminate the redundant blocks.

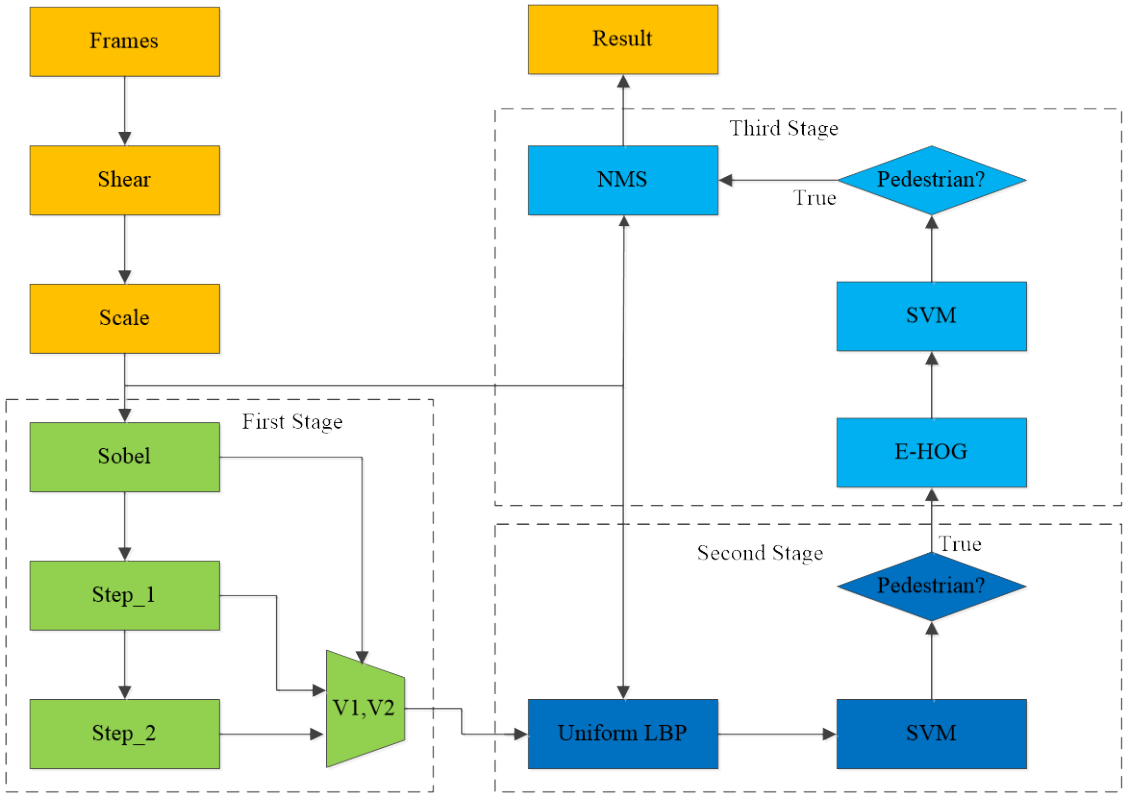

Figure.4 Block diagrams of Pedestrian detection

III. REAL-TIME PEDESTRIAN DETECTION ON BOARD

3.1 Accelerator of E-HOG IP

E-HOG is the key module in pedestrian detection system as the feature descriptor. Because of

infinite source, E-HOG is design as hardware core, calling E-HOG IP. Meanwhile, the E-HOG IP can be used to detect or track objects, such as animals, cars and so on. The modules of E-HOG IP mainly include gradient calculation (GRA module), magnitude and orientation generation (M&A module), tri-linear interpolation (TRI module). Except these key models, there are some assisted modules for E-HOG IP, such as PRE and CON module.

'Data_in' is the 8 bit inputting pixels; 'Ready_in' and 'Rst' is the 1 bit control signal separately. In the output terminal, 'Data_out' is the 16 bit E-HOG feature. 'Ready_out' is also the 1-bit control signal, which stands for the ready of 'Data_out'.

One 256x32bits single port SRAM is required. Because the data stored in the SRAM is generated discretely, the memory-size 256x32 is just proper for this integrate circuits. In the output of E-HOG, the width of data is 16bit. Then, 32bit features will be divided into high 16 bit and low 16bit. One 32bit E-HOG feature will be transmitted into the FPGA in two clock cycles.

3.2 Real-time vehicle equipment of pedestrian detection

In order to decrease hardware overload and improve detection speed, the vehicle equipment is self-developed as Figure.5 showed.

Through two independently boards, the backboard and core board can be extended to the other functions. The core board contains one FPGA, two SDRAMs, one flash and some other devices.

The center device in core board is Cyclone Ⅲ.The other devices are MT9M111, one SRAM, one crystal, power and interfaces for debugging and downloading program. At the same time, E-HOG IP is embedded into system on the backboard. The connection between backboard and core board is SODIMM-200.

Based on the structure of Figure.5, the modules of pedestrian detection system are showed in Figure.6. Pedestrian detection system are constructed with the Receive module, Data buffer module , first stage module, second stage module ,third stage module , NMS module , MT9M111 module, SRAM module and DVI module. In the backboard, one SDRAM is also used to store the data.

The frames are firstly acquired by camera, which is the MT9M111 of MICRON. The 1280x1024 pixels can’t work well because of the huge data. So, the image size from MT9M111 is 640x480 pixels. I2C_config, CCD_CAPTURE and CCD_to_RGB modules are used to receive the pixel values from MT9M11. Two SDRAMs on the core board and one SDRAM on the backboard have

different functions. Because of the graying image are used in the FPGA many times, the graying data stores to SDRAM in core board, which is labeled SDRAM_1. And the Red, Green and Blue data from MT9M11 are stored to SDRAM in backboard, which is labeled SDRAM_2.

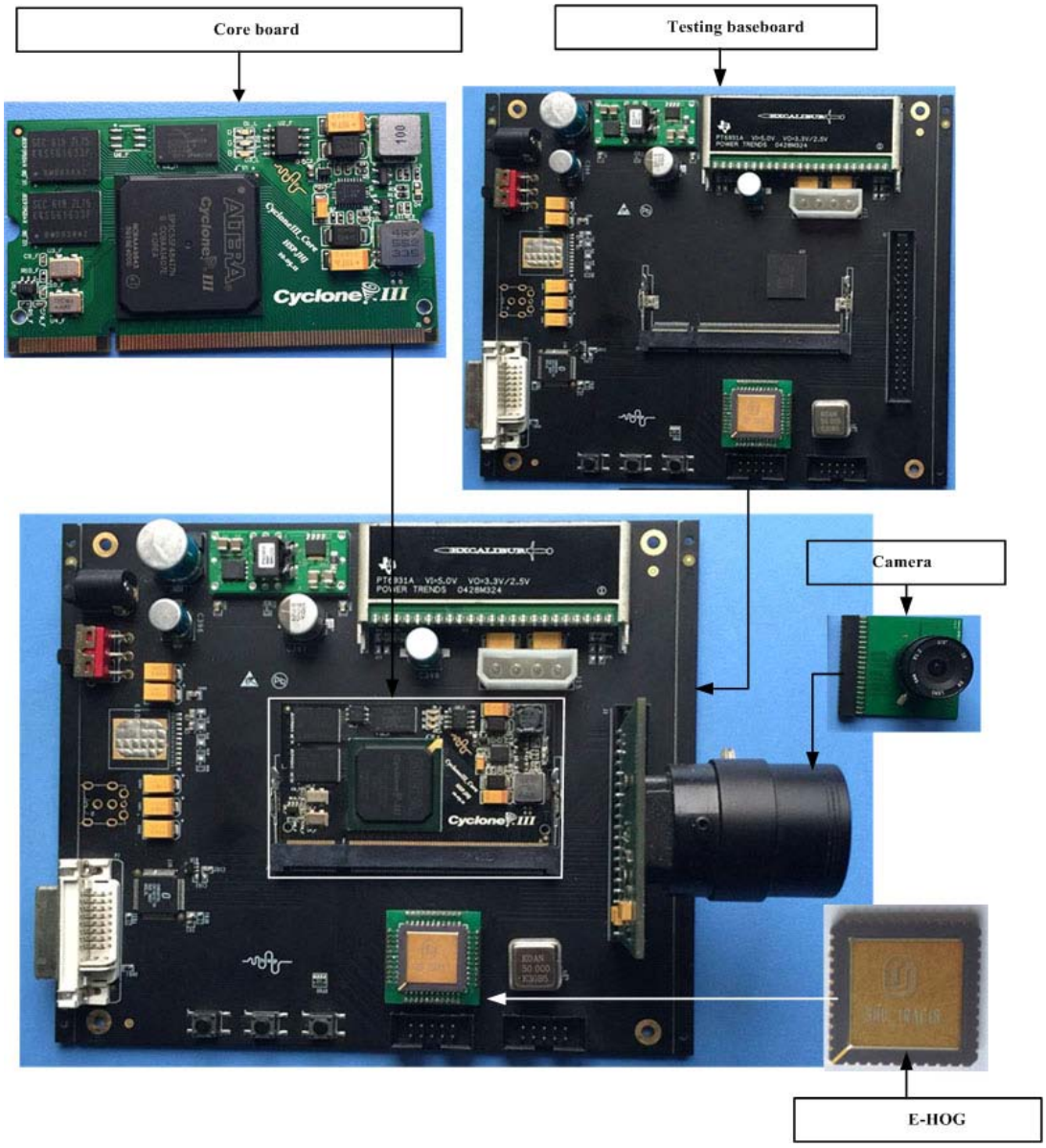

Figure.5 Actual object picture

In order to decrease the calculation of Uniform LBP detection window, the 'time for space' is used to store all Uniform LBP features to SDRAM. The second stage can’t calculate all detection windows in one time. So, the location of detection windows will be stored to SDRAM_2. At the

same time, the LBP features are reading from the SDRAM_3 and calculate with SVM.

Because of infinite source of hardware, this pedestrian detection system will be cost about 97% hardware overload of FPGA without using E-HOG IP. So E-HOG IP is developed into the integrated circuits as hardware accelerator.

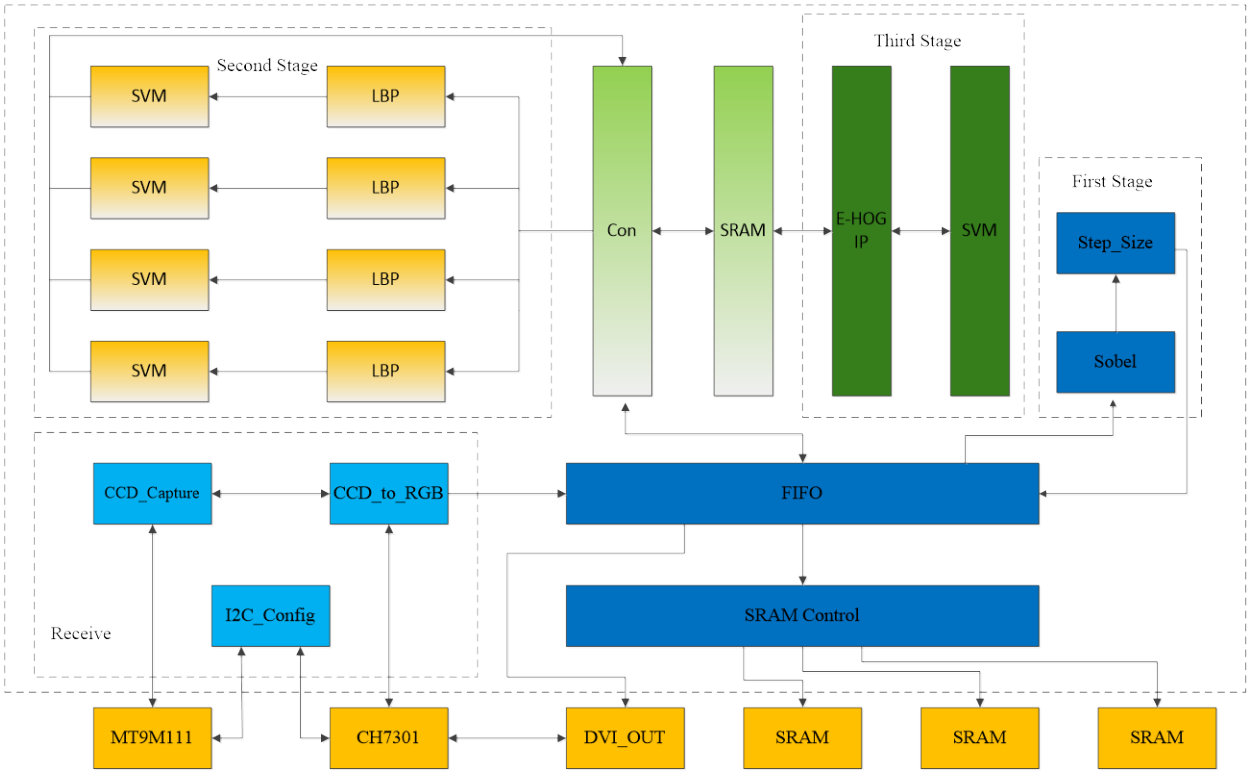

Figure.6 Pedestrian detection on board

IV. Evaluation of performance of pedestrian detection system

In order to evaluate the performance, three methods: Matlab, FPGA and ASIC, are used. The video (640x480 pixels) is acquired by camera about 40 minutes to detect pedestrians. Because this system justly is the model devices, the camera of pedestrian detection is to detect the pedestrians across the screen. Except the evaluation performance of pedestrian detection system, the evaluation of E-HOG is also made.

4.1 Evaluation of E-HOG IP

The evaluation of integrated circuits IP are chosen by FPGA and ASIC separately. Firstly, the E-HOG is realized on the FPGA-Cyclone III. Table 1 lists the hardware overload using FPGA with the E-HOG IP. Table 2 lists the result report of traditionally HOG from the Dollar's paper.

From the Table 1 and Table 2, the E-HOG can decrease 23.4% hardware cost than the traditionally HOG. The memory size just has the one third memory size of traditionally HOG. Except the evaluation using FPGA, another method is to evaluate the performance using ASIC. Additionally, this IP is developed with ceramic leaded chip carrier (CLCC44), type chip of 1cm×1cm, based on the 180nm, 1-poly/4-metal CMOS logic process. This ASIC IP is labeled SHU-IRAC18. SHU-IRAC18 contains one test chain using the technology of design for test (DFT). About the test memory size, simple coding is wrote for testing whether SRAM is right or not. So, this coding doesn't have the repaired function.

Table 1 FPGA synthesis result Report

Slice logic	**Used**	**Utilization (%)**
Number of slice registers	3551	22
Total Combination function	6313	41
Total Memory bits	5120	1

Table 2 Traditionally HOG FPGA Report

Slice logic	**Used**	**Utilization (%)**
Number of slice registers	4657	22
Total Combination function	8156	41
Total Memory bits	16384	2

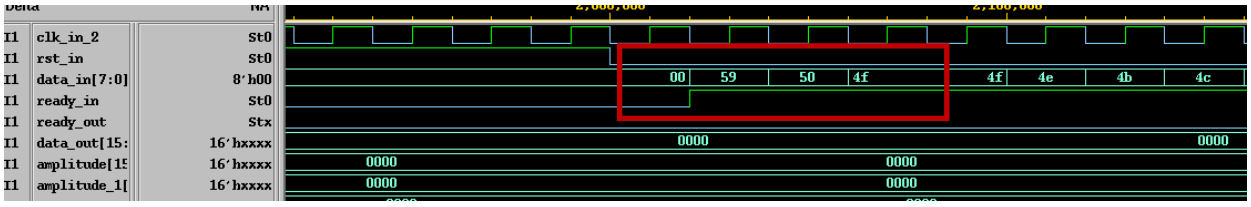

Figure.7 Input signal

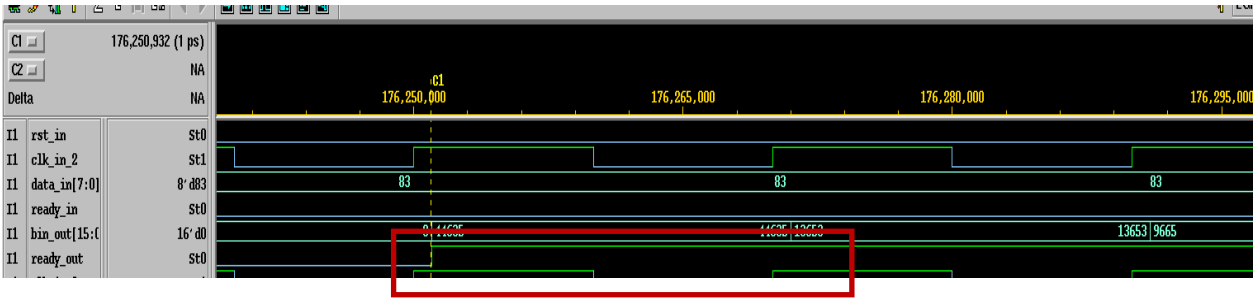

Figure.8 Output signal

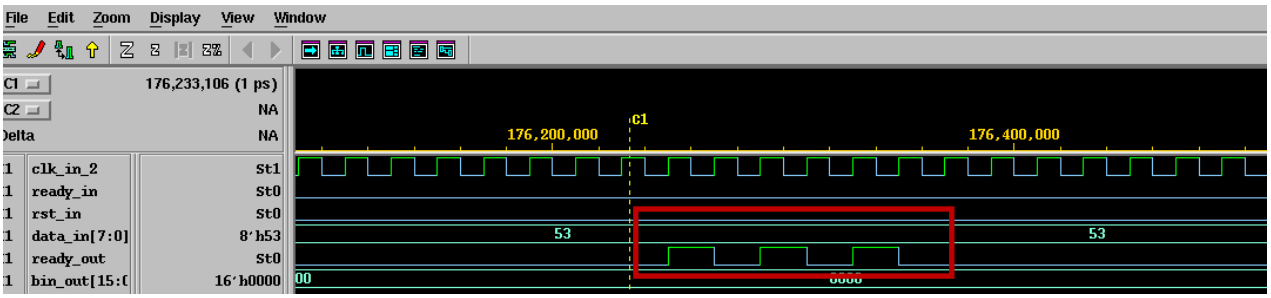

Figure.9 Abnormal input and Regular output

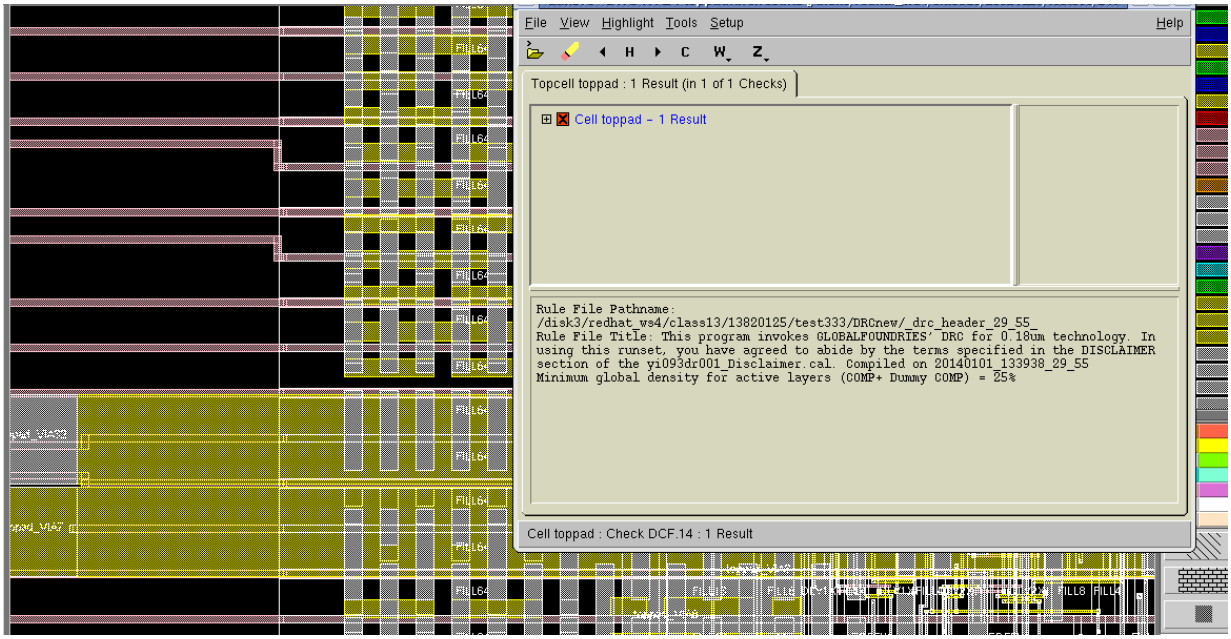

Figure.10 DRC result of E-HOG Layout

Figure.11 E-HOG IP

Figure.7~Figure.9 shows the VCS simulation results of the E-HOG IP. Figure.10 exhibits the DRC result of E-HOG IP Layout. Fig.11 shows the object of E-HOG IP. In order to test the function of E-HOG IP, the FPGA connects E-HOG IP through Signal Tap II for stimulating the E-HOG IP to work. The Power consumption of SHU-IRAC18 is 98mW. The results show that the E-HOG IP works very well and can be used as the hardware IP to extract the pedestrian feature.

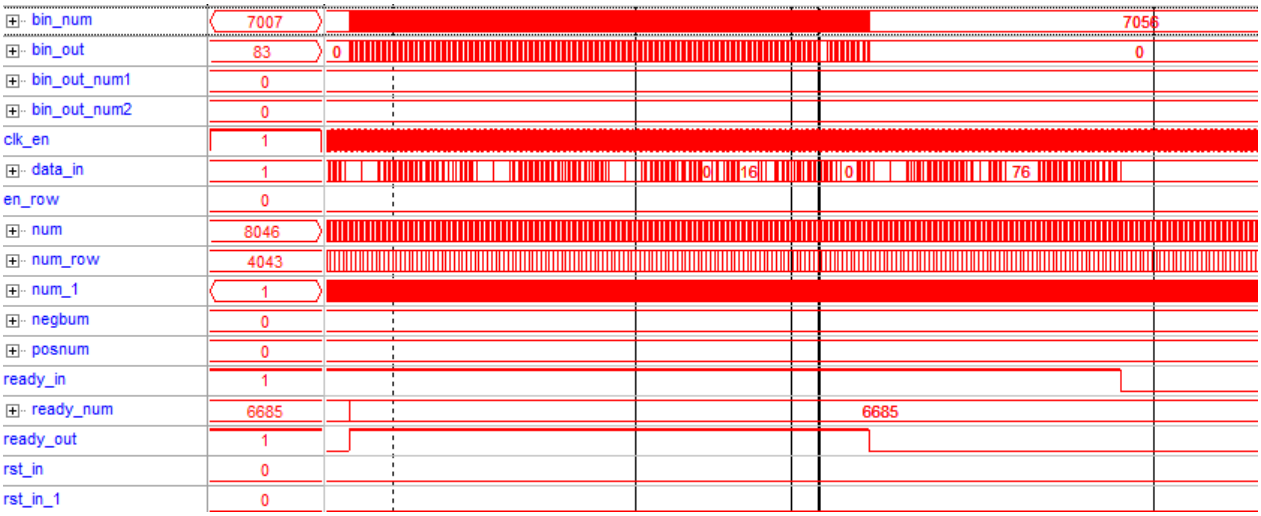

Figure12. E-HOG IP Waveform

4.2 Evaluation of pedestrian detection system

Evaluation of pedestrian detection system are used two methods: 1) FFPI (detection rate VS False Positive Percent Image) [19] [20] [21] [22] [23] [24] ; 2) processing time. There exist about 16 kinds of representative feature using to detect pedestrians. The HOG and HOG-LBP in this paper are both the state of art features for evaluation performance. Before evaluating, the pedestrian detection data sets must be chosen. It is well-known that INRIA dataset is the first and frequency

used dataset for evaluating the performance of algorithms. INRIA dataset contains 'train_64x128_H96' and 'test_64x 128_H96' as images to train linear SVM and test the performance. Then, INRIA dataset is the baseline set. But the INRIA data sets contain the background, which sometimes don't accord with the domestic. Except INRIA data sets, some images are still gathered to match domestic background and evaluate the performance of algorithm. From the Figure.13, the three stages detector (Lbp-hog in Figure.13) outperforms the HOG detector across all FPPI values.

Through the Sobel operator, location of detection window can be fixed. The traditionally detection window slides allover one image according to "coarse-to-fine" method. The coarse step is 16 pixels. The fine step is 8 pixels. In one 640x480 pixels, the number of detection window is (640-16/16) x (480-16/16) according the exhaustive search; But the number of detection window, which uses the Sobel, is 73. The results shows that the Sobel operator can decrease the calculation and improve the detection speed.

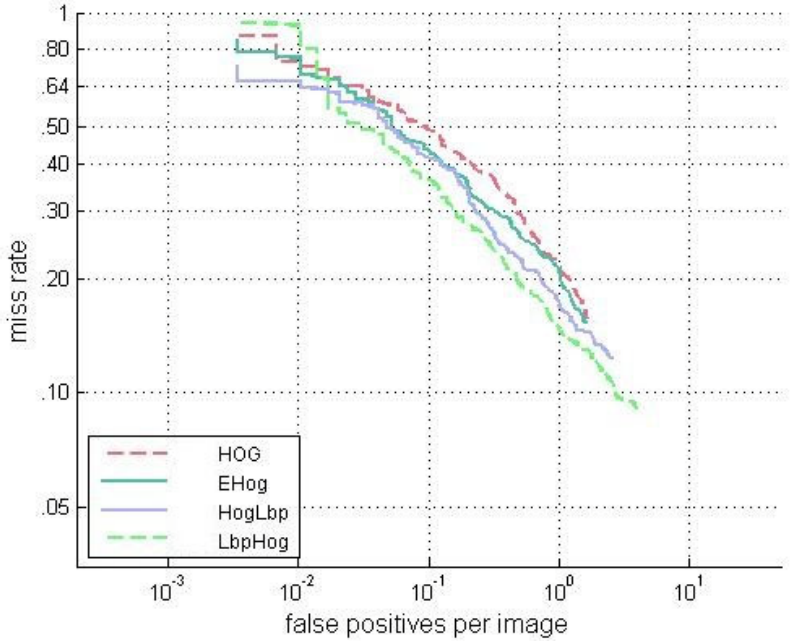

Figure.13 Performance of E-HOG and Sobel-LBP-E-HOG

Table 3 lists the processing time of different methods: HOG, E-HOG, LBP-HOG and Our method. From the Table 3, we can see that the three stages can be used about 32ms, which satisfy the real-time.

Table 3 Processed of Time

Algorithms	Time (ms)
HOG	686
E-HOG	411
HOG-LBP	180
Three Stage(our)	27

4.3 The evaluation of pedestrian detection system

Figure.14 and Figure.15 exhibit the vehicle equipment of pedestrian detection system with E-HOG IP. The camera in vehicle equipment is Lens 4mm working under 54 Mhz, while the frequency from the crystal oscillator can be replaceable for E-HOG IP.

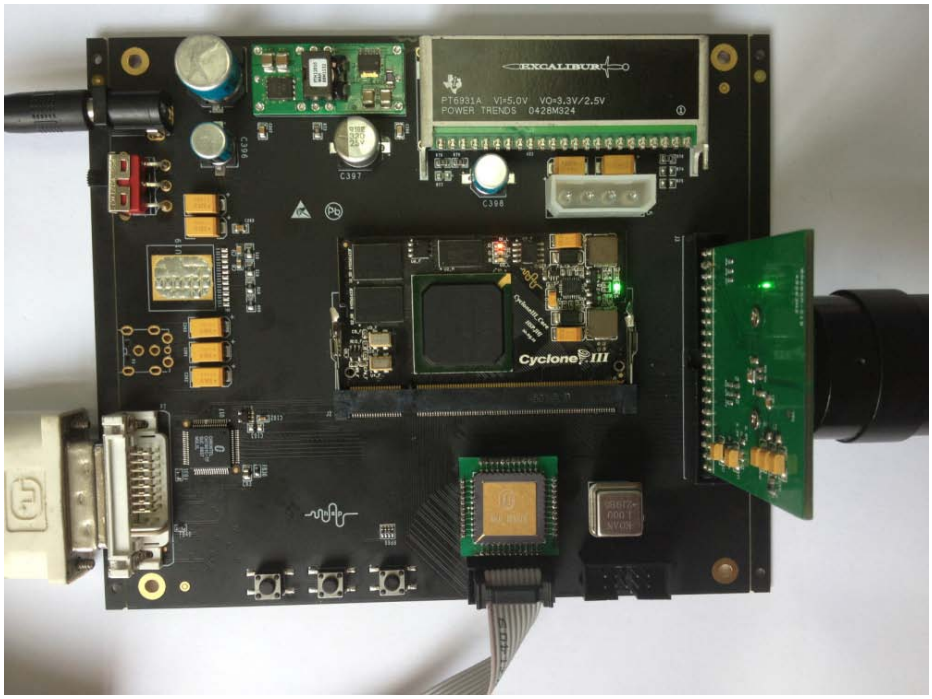

Figure.14 Vehicle equipment of pedestrian detection

Figure.15 Evaluation of experiment

When the pedestrian detection system begins to work, the green LED on board will be burned. The video is captured by the tachograph and lasted about 40 minutes to evaluate the performance of vehicle equipment.

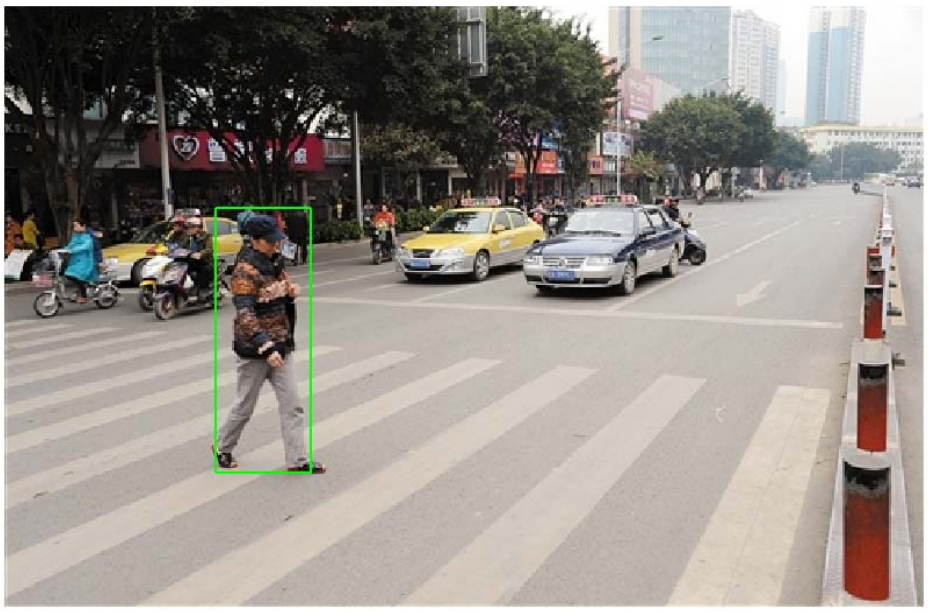

(a)

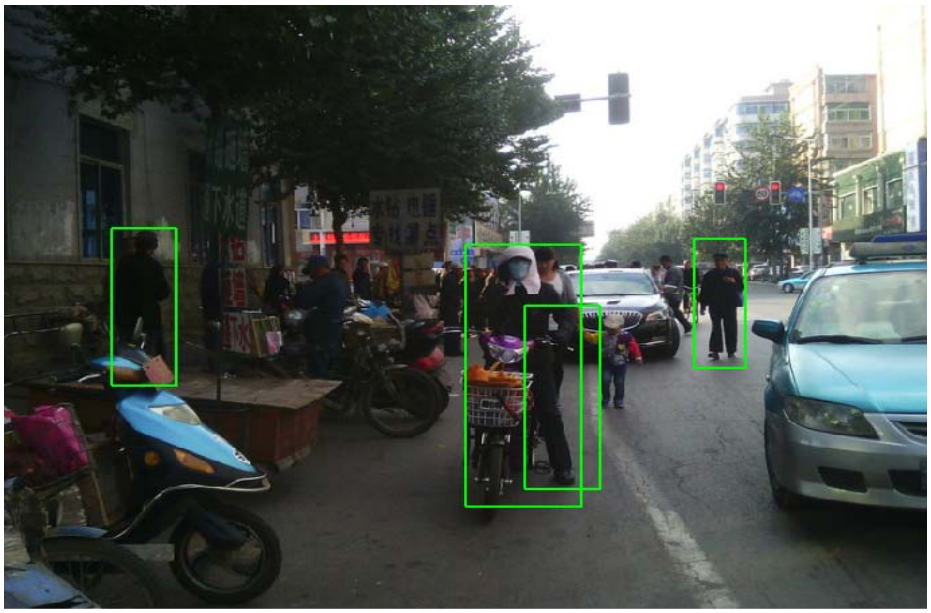

（b）

Figure.16 Partial results of pedestrian detection

Figure.16 shows the partial results of pedestrian detection system. The Sobel operator calculates the sliding steps, which can decrease the 60% calculation of the system, compared with the traditionally methods. This is the biggest characteristic of this pedestrian detection system. The first and second stage can remove about 95% non-pedestrian zone through simple calculation. The second stage transfer the ROIs to the E-HOG in third stage is just two or three detection windows more than the pedestrians in reality.

In the hardware, the crystal of E-HOG IP can be changed. When the frequency of crystal is 80Mhz, this pedestrian detection can process 15 fps. But the fact is that the hardware platform of pedestrian detection just chooses Cyclone III as the center unit, with one E-HOG IP. Then, this pedestrian detection can process 30 fps with 160 Mhz based on the existing results of experiment. If a couple of the E-HOG IPs is paralleled on the hardware structure, the detection speed can be faster than the 30 fps. This detection speed can satisfy the demand of real-time.

V. CONCLUSION

This thesis discusses a unify structure for pedestrian detection system to solve detection speed. The Sobel algorithm is used to calculate the sliding step of detection window of Uniform LBP.

Then the process time can be decrease to 1/128 at some zones in image. After determines the step of detection window, the second stage is used to extract the ROIs, which may be exist the pedestrian detection, through Uniform LBP based on the Linear-SVM. The third stage is to give the finally results whether pedestrian zone or not. In the last, NMS mixtures more labels to one. The E-HOG IP is used as the accelerator for pedestrian detection. Without using GPU or CPU, this system on board can deal with 30 fps when E-HOG IP works with 160 MHz. So, this vehicle equipment can be used as the real-time pedestrian detection system.

ACKNOWLEDGMENTS

This work is supported by the National Natural Science Foundation of China (Grant: 61376028).

REFERENCES

[1] Hosang J, Benenson R, Dollar P, et al., “What makes for effective detection proposals”, IEEE Transactions on Pattern Analysis & Machine Intelligence, Vol.38, No.4, 2016, pp. 814-830.

[2] Benenson R, Omran M, Hosang J, et al., “Ten Years of Pedestrian Detection, What Have We Learned?” Computer Science, Vol. 8926, 2014, pp. 613-627.

[3]Tuzel O, Porikli F, Meer P., “Pedestrian detection via classification on Riemannian manifolds”, Pattern Analysis and Machine Intelligence, IEEE Transactions on, Vol. 30, No.10, 2008, pp. 1713-1727.

[4] Park K Y, Hwang S Y., “An improved Haar-like feature for efficient object detection”, Pattern Recognition Letters, Vol. 42, No.1, 2014, pp.148-153.

[5] Liu Y, Yao J, Xie R, et al. Pedestrian detection from still images based on multi-feature covariances// IEEE International Conference on Information and Automation. IEEE, 2013:614-619.

[6]Dalal N, Triggs B., “Histograms of oriented gradients for human detection,”//Computer Vision and Pattern Recognition, 2005.CVPR 2005.IEEE Computer Society Conference on. IEEE, 2005, 1: 886-893.

[7] Wanli O, Xingyu Z, Xiaogang W., “Single-Pedestrian Detection Aided by Two-Pedestrian Detection”, Pattern Analysis & Machine Intelligence IEEE Transactions on, vol.37, no. 4, 2015, pp.1875-1889.

[8] Liang F, Tang S, Wang Y, et al. “A Sparse Coding Based Transfer Learning Framework for Pedestrian Detection”, Advances in Multimedia Modeling. 2013:272-282.

[9] Szarvas M, Yoshizawa A, Yamamoto M, et al. “Pedestrian detection with convolutional neural networks”, Intelligent Vehicles Symposium, 2005. Proceedings. IEEE. 2005:224-229.

[10] Bilal M, Khan A, Khan M U K, et al. “A Low Complexity Pedestrian Detection Framework for Smart Video Surveillance Systems”, IEEE Transactions on Circuits & Systems for Video Technology, 2016:1-1.

[11]Maji S, Berg A C, Malik J. “Classification using intersection kernel support vector machines is efficient”, Computer Vision and Pattern Recognition, 2008. CVPR 2008. IEEE Conference on. IEEE, 2008: 1-8.

[12] Wang Y, Liu X. “Face recognition based on improved support vector clustering”, Internati-onal Journal on Smart Sensing and Intelligent Systems, vol. 7, no.4, 2014,pp.1807-1829.

[13] Shibayama Y, Kim H K, Fujimura K, et al., “On-board Pedestrian Detection by the Motion and the Cascaded Classifiers”, International Journal of Intelligent Transportation Systems Research, vol.9 no.3, 2011,pp.101-114.

[14]Benenson R, Mathias M, Timofte R, et al., “Pedestrian detection at 100 fps”, Computer Vision and Pattern Recognition (CVPR), 2012 IEEE Conference on. IEEE, 2012: 2903-2910.

[15]Bauer S, Köhler S, Doll K, et al., “FPGA-GPU architecture for kernel SVM pedestrian detection”, Computer Vision and Pattern Recognition Workshops (CVPRW), 2010 IEEE Computer Society Conference on. IEEE, 2010:61-68.

[16] Guo Z, Zhang L, Zhang D. “Rotation invariant texture classification using LBP variance (LBPV) with global matching”, Pattern Recognition, vol. 43,no. 3, 2010, pp. 706-719.

[17]Wang X, Han T X, Yan S. “An HOG-LBP human detector with partial occlusion handling”, Computer Vision, 2009 IEEE 12th International Conference on. IEEE, 2009: 32-39.

[18] Margae S E, Kerroum M A, Fakhri Y., “ Fusion of Local and Global Feature Extraction Based on Uniform LBP and DCT for Traffic Sign Recognition”, 2015, 10(1).

[19] Murat Alçin, İhsan Pehlivan, İsmail Koyuncu. “Hardware Design and Implementation of a Novel ANN-based Chaotic Generator in FPGA”, Optik - International Journal for Light and Electron Optics, vol. 127, no. 132016, pp. 5500-5505.

[20] Liu Y, Zou L, Li J, et al. “Segmentation by weighted aggregation and perceptual hash for pedestrian detection”, Journal of Visual Communication & Image Representation, vol. 36, 2016, pp. 80-89.

[21]Lee, Chung-Hee, Kim, Dongyoung, “Improvement of processing time for stereo vision-based pedestrian detection”, Proceedings of HCI Korea. Hanbit Media, Inc., 2016.

[22]Ouyang W, Zeng X, Wang X, “Learning Mutual Visibility Relationship for Pedestrian Detection with a Deep Model”, International Journal of Computer Vision, 2016:1-14.

[23]Domonkos Varga, Tamás Szirányi, “Robust real-time pedestrian detection in surveillance videos”, Journal of Ambient Intelligence and Humanized Computing, 2016:1-7.

[24]Qi B, John V, Liu Z, et al. “Pedestrian detection from thermal images: A sparse representation based approach”, Infrared Physics & Technology, vol. 76, 2016, pp.157-167.